Astrophysics of gravitational wave sources

Lecture 10: Final phases of stellar evolution

Ondřej Pejcha

ÚTF MFF UK

The Astrophysical Journal, 893:133 (8pp), 2020 April 20 https://doi.org/10.3847/1538-4357/ab7f2c

On Stellar Evolution in a Neutrino Hertzsprung–Russell Diagram

Ebraheem Farag[1], F. X. Timmes[1,2], Morgan Taylor[1], Kelly M. Patton[3], and R. Farmer[4]
[1] School of Earth and Space Exploration, Arizona State University, Tempe, AZ 85287, USA; ekfarag@asu.edu
[2] Joint Institute for Nuclear Astrophysics—Center for the Evolution of the Elements, USA
[3] Department of Physics and Astronomy, Colby College, Waterville, ME 04961, USA
[4] Anton Pannenkoek Institute for Astronomy and GRAPPA, University of Amsterdam, NL-1090 GE Amsterdam, The Netherlands
Received 2019 November 26; revised 2020 March 4; accepted 2020 March 10; published 2020 April 23

Abstract

We explore the evolution of a select grid of solar metallicity stellar models from their pre-main-sequence phase to near their final fates in a neutrino Hertzsprung–Russell diagram, where the neutrino luminosity replaces the traditional photon luminosity. Using a calibrated MESA solar model for the solar neutrino luminosity ($L_{\nu,\odot} = 0.02398 \cdot L_{\gamma,\odot} = 9.1795 \times 10^{31}$ erg s^{-1}) as a normalization, we identify $\simeq$0.3 MeV electron neutrino emission from helium burning during the helium flash (peak $L_\nu/L_{\nu,\odot} \simeq 10^4$, flux $\Phi_{\nu,\mathrm{He\ flash}} \simeq 170\ (10\ \mathrm{pc}/d)^2$ cm^{-2} s^{-1} for a star located at a distance of d parsec, timescale $\simeq$3 days) and the thermal pulse (peak $L_\nu/L_{\nu,\odot} \simeq 10^9$, flux $\Phi_{\nu,\mathrm{TP}} \simeq 1.7 \times 10^7\ (10\ \mathrm{pc}/d)^2$ cm^{-2} s^{-1}, timescale $\simeq$0.1 yr) phases of evolution in low-mass stars as potential probes for stellar neutrino astronomy. We also delineate the contribution of neutrinos from nuclear reactions and thermal processes to the total neutrino loss along the stellar tracks in a neutrino Hertzsprung–Russell diagram. We find, broadly but with exceptions, that neutrinos from nuclear reactions dominate whenever hydrogen and helium burn, and that neutrinos from thermal processes dominate otherwise.

Single star evolution before core-collapse

Central temperature and pressure

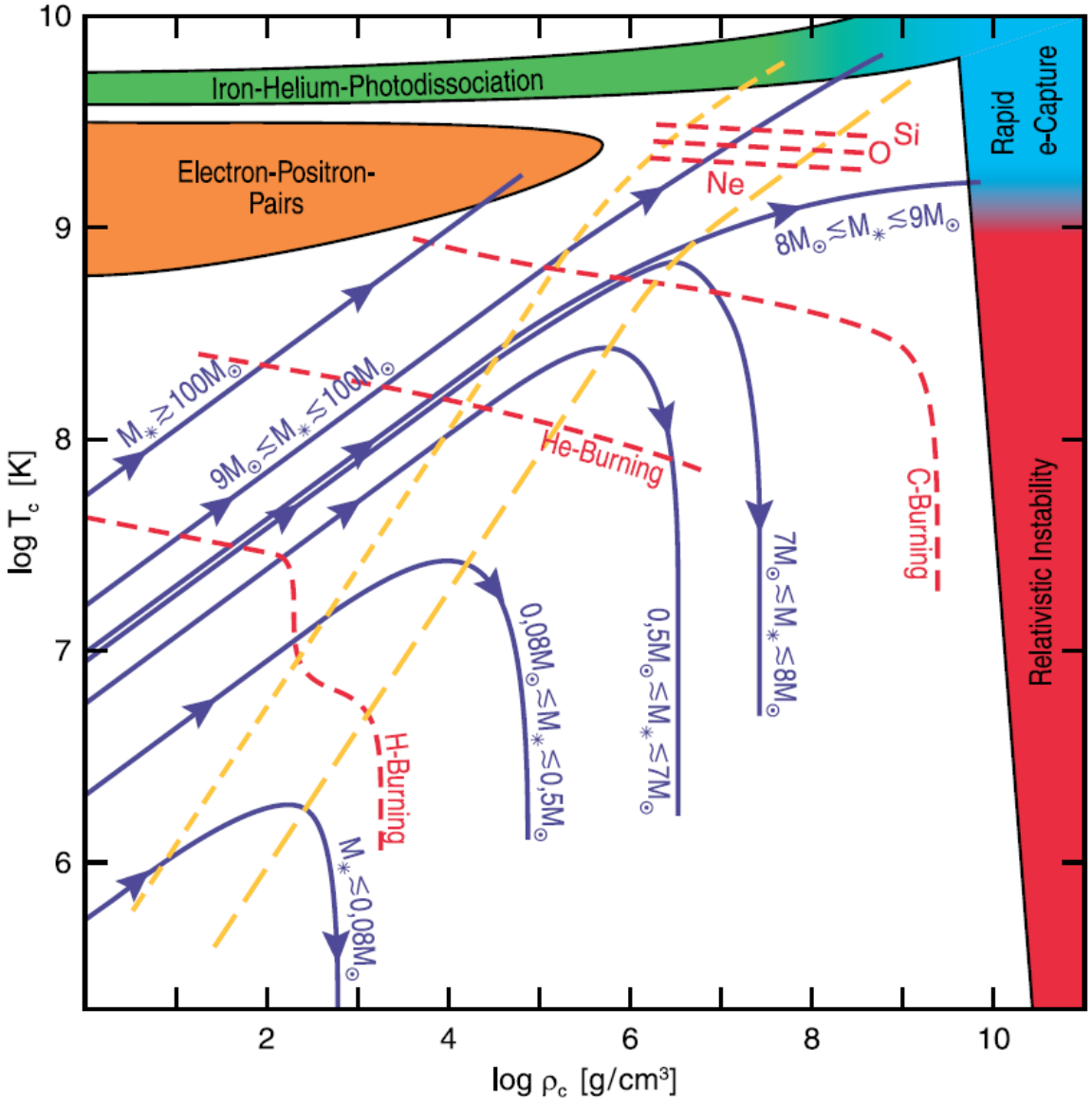

Janka (2012)

1 erg = 10^{-7} J

Massive star death

$1\ L_\odot = 3.9 \times 10^{33}$ ergs/s

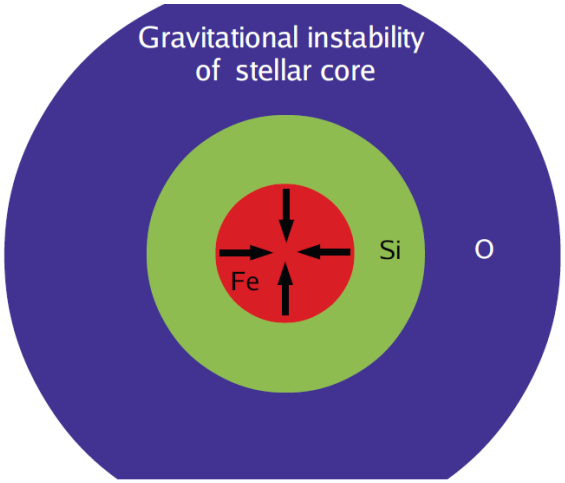

$M_{initial} > 8\ M_\odot$
Collapse from WD size ~0.3s

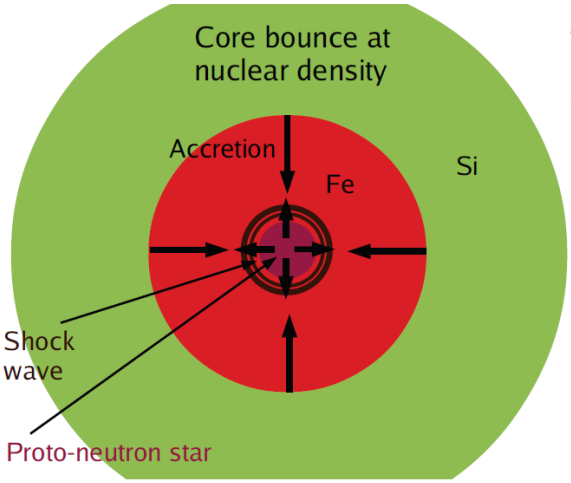

Proto-neutron star ~60 km
Binding energy ~ 3×10^{53} ergs

<10m
s

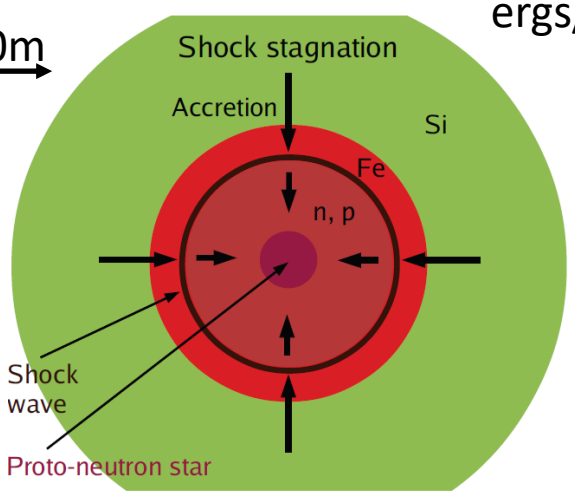

Stalled shock at 100-200 km
Neutrino cooling ~ 10^{52} ergs/s
Duration up to ~1 s

Reason not fully understood

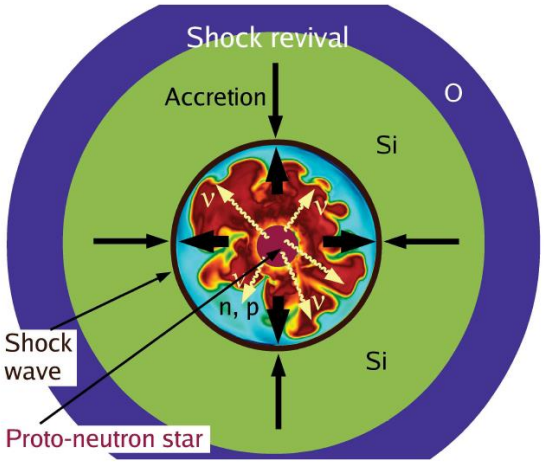

All NS binding energy released
before 10-100s

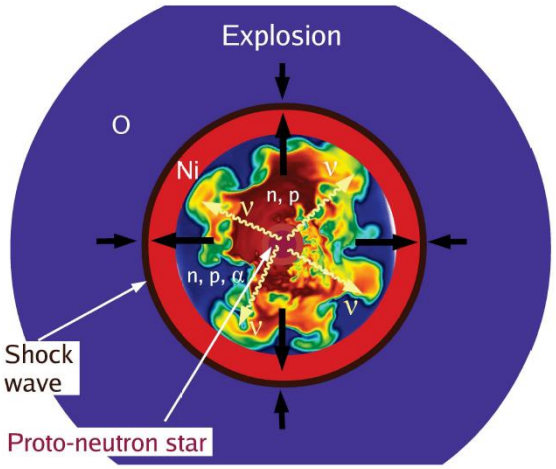

Explosion energy ~10^{51} ergs
10^{-3} – 10^{-1} $M_\odot$ of Nickel-56
Shock at surface in ~hours

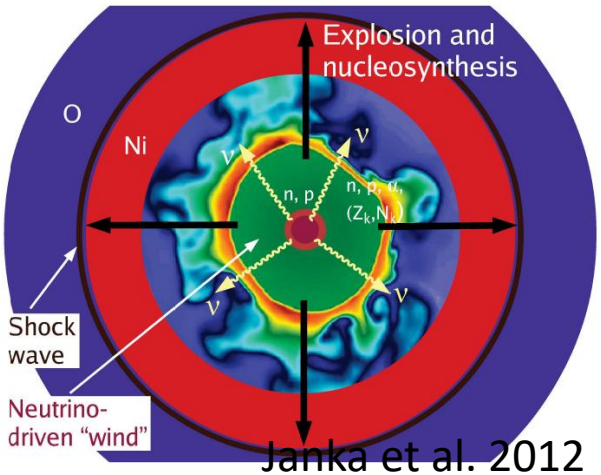

Janka et al. 2012


4GIFs
.com

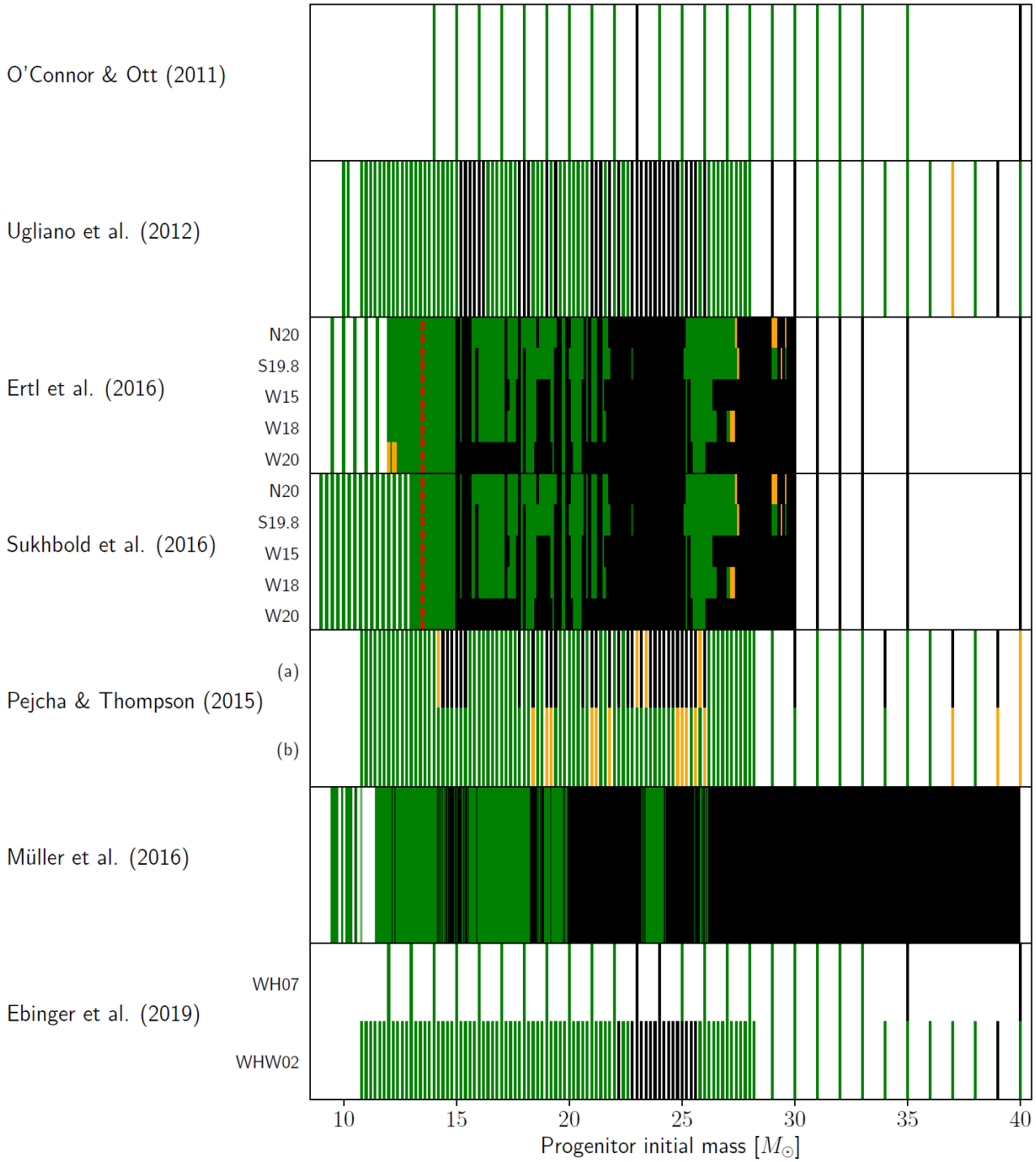
O'Connor & Ott (2011)
Ugliano et al. (2012)
Ertl et al. (2016)
N20
S19.8
W15
W18
W20
Sukhbold et al. (2016)
N20
S19.8
W15
W18
W20
Pejcha & Thompson (2015)
(a)
(b)
Müller et al. (2016)
Ebinger et al. (2019)
WH07
WHW02
10
15
20
25
30
35
40
Progenitor initial mass [$M_\odot$]

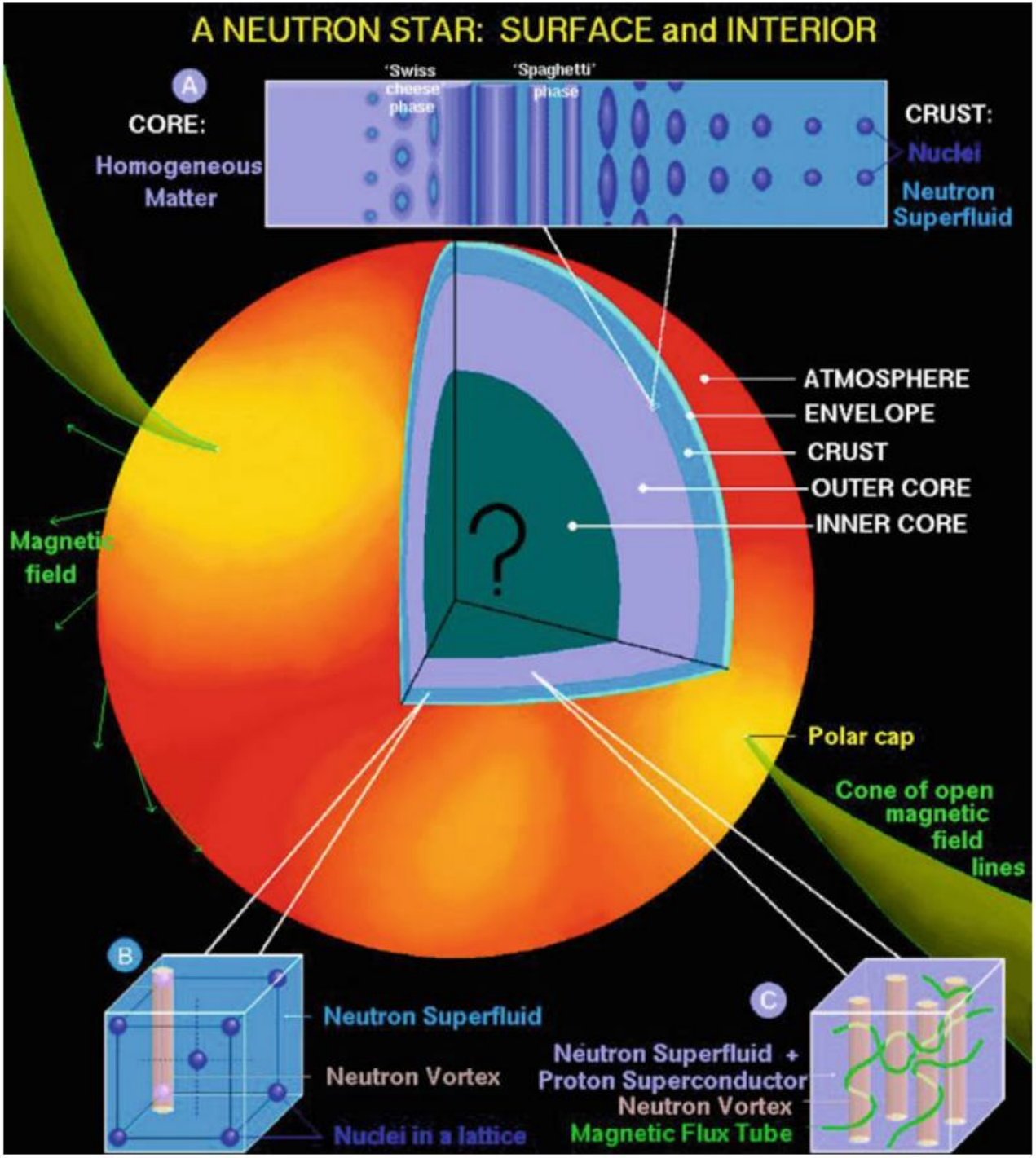
A NEUTRON STAR: SURFACE and INTERIOR
A
CORE:
Homogeneous Matter
'Swiss cheese' phase
'Spaghetti' phase
CRUST:
Nuclei
Neutron Superfluid
ATMOSPHERE
ENVELOPE
CRUST
OUTER CORE
INNER CORE
?
Magnetic field
Polar cap
Cone of open magnetic field lines
B
Neutron Superfluid
Neutron Vortex
Nuclei in a lattice
C
Neutron Superfluid +
Proton Superconductor
Neutron Vortex
Magnetic Flux Tube

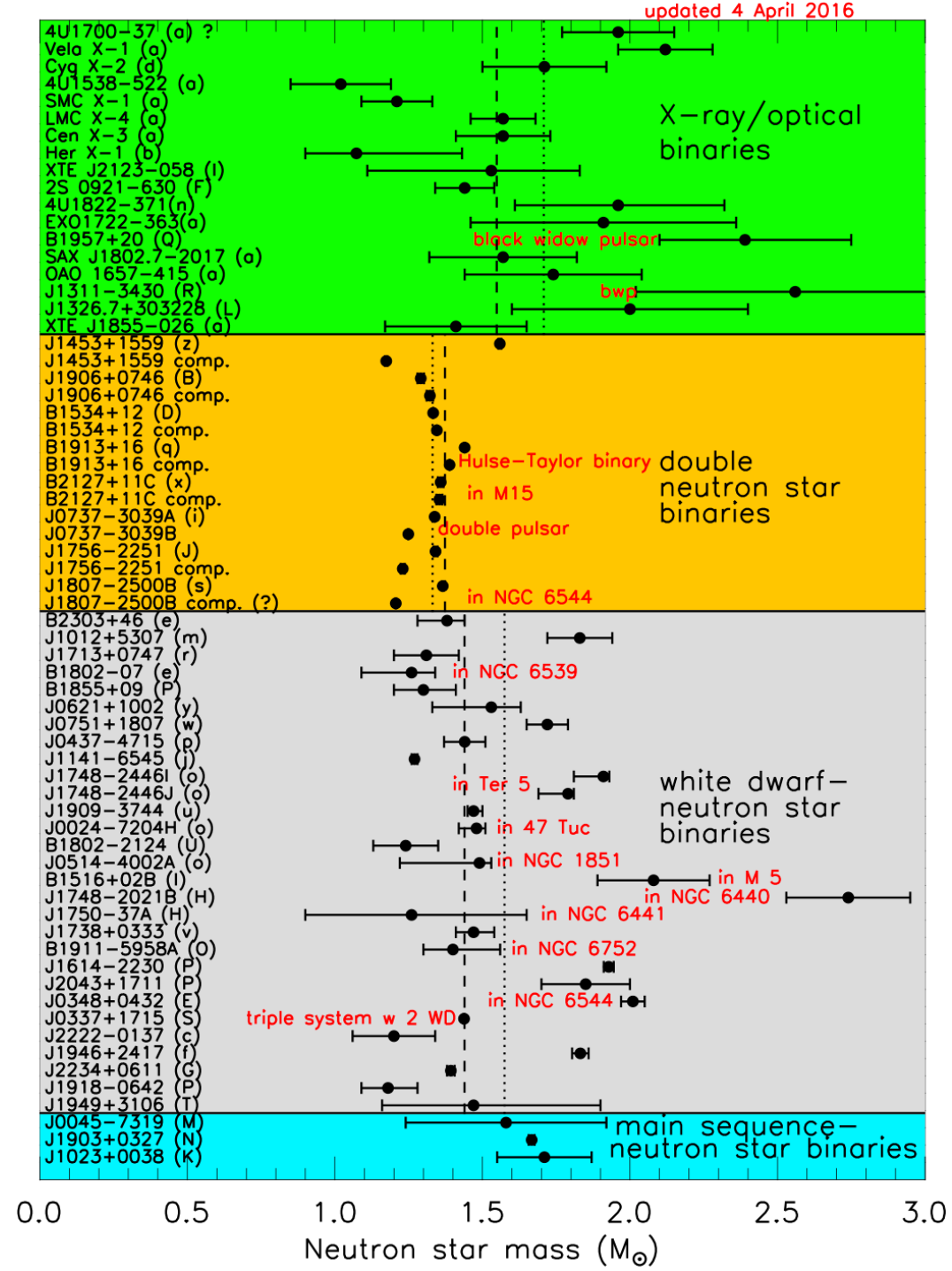

https://stellarcollapse.org/nsmasses.html

Single star evolution before core-collapse

Central temperature and pressure

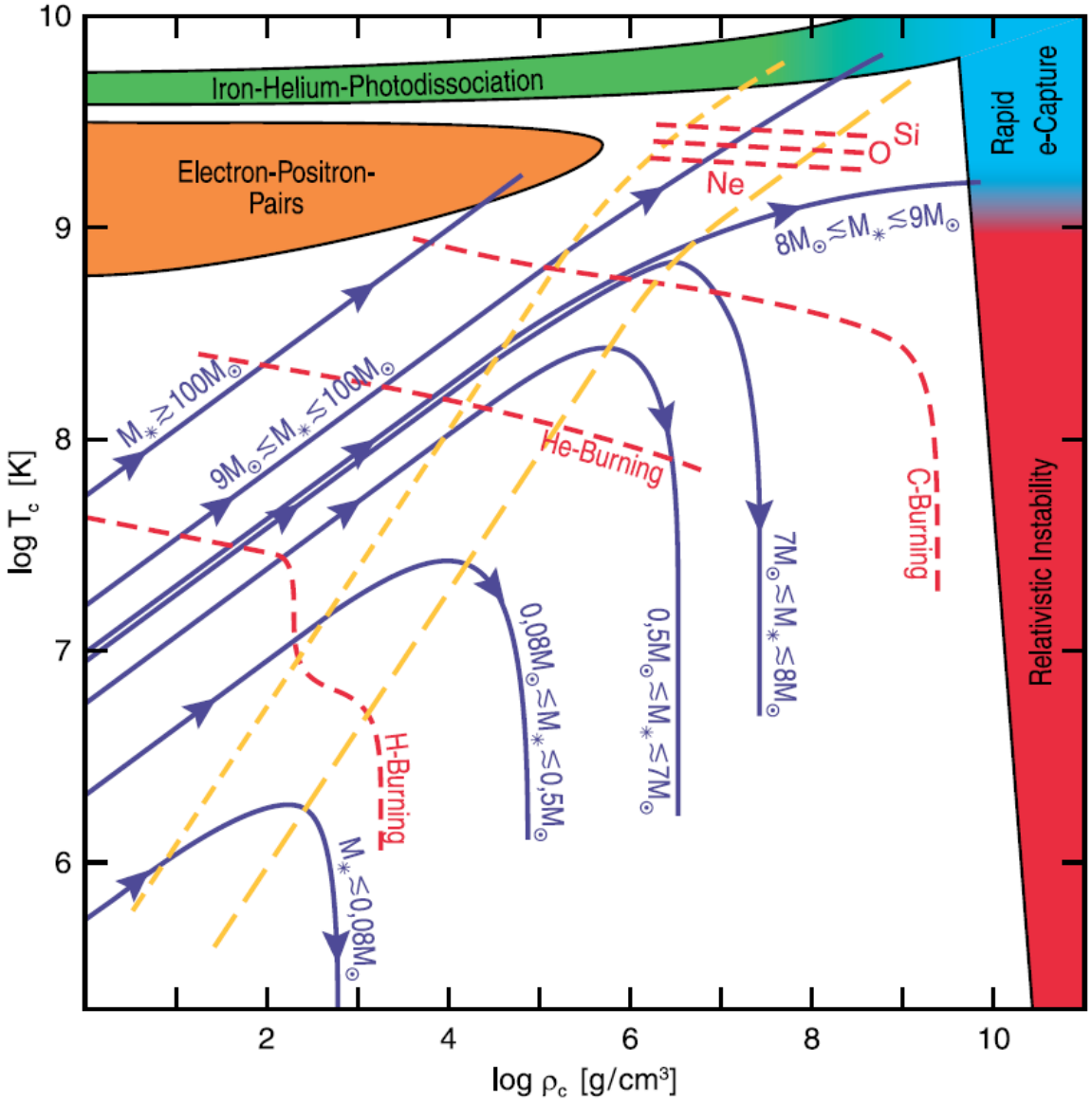

Janka (2012)

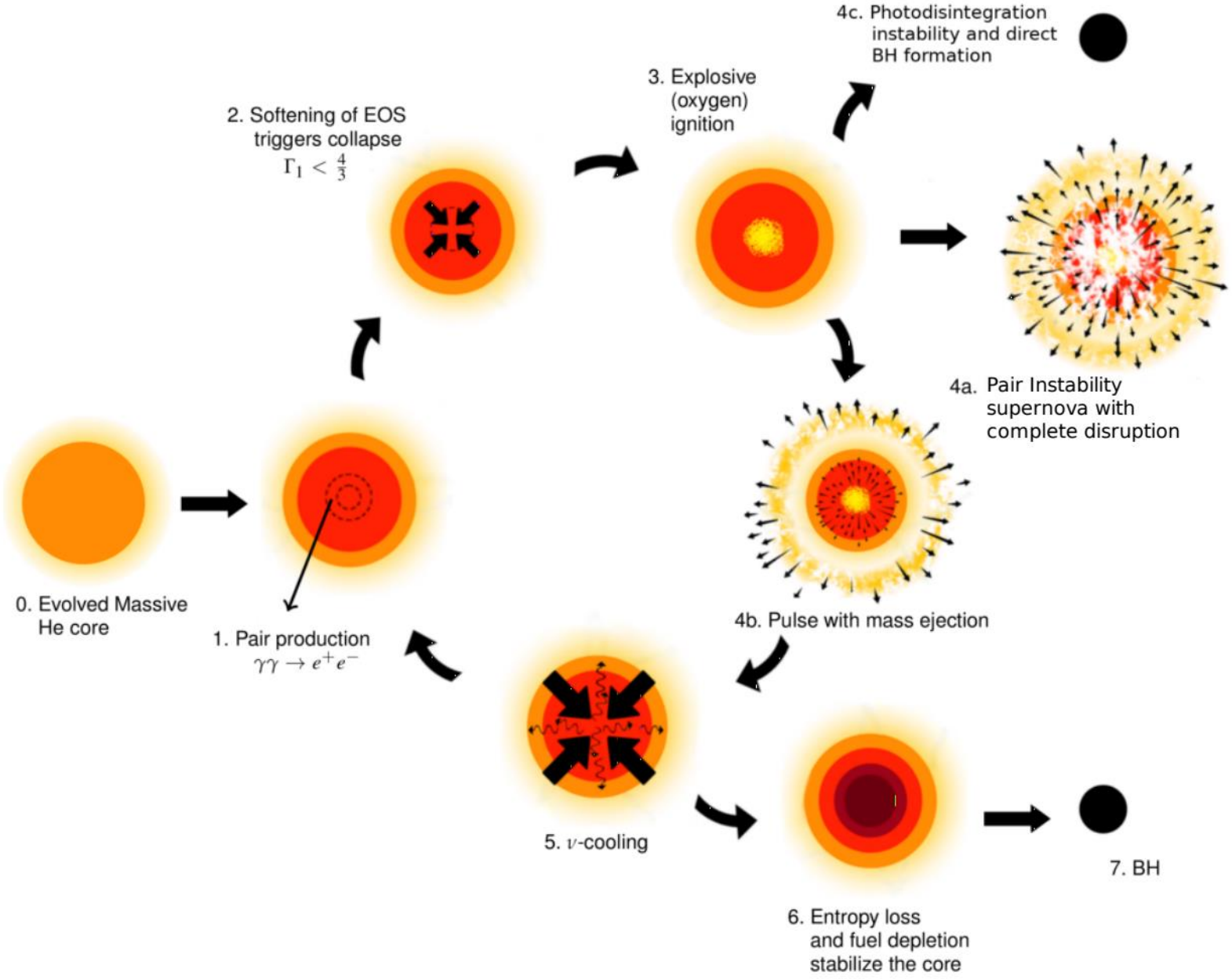

Renzo et al. (2020)

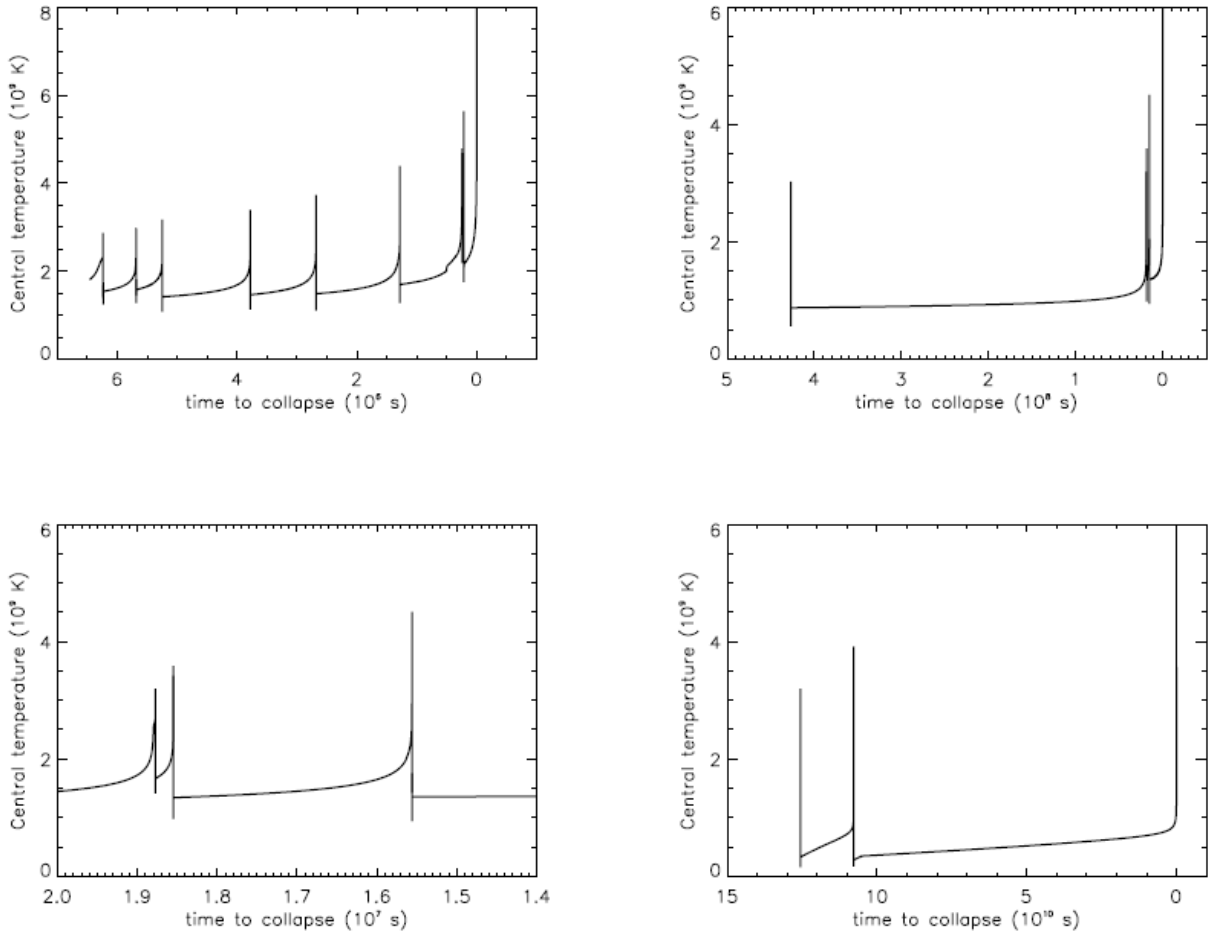

Fig. 2 Pair-driven pulsations cause rapid variations in the central temperature (10^9 K) near the time of death for helium cores of 32, 36, 40, 44, 48, 52 (on two different time scales) and 56 $M_\odot$ (left to right; top to bottom). The log base 10 of the time scales (s) in each panel are respectively 4, 4, 5, 5, 6, 8, 7, and 10. The last rise to high temperature marks the collapse of the iron core to a compact object. More massive cores have fewer, less frequent, but more energetic pulses. All plots begin at central carbon depletion.

Woosley & Heger (2015)

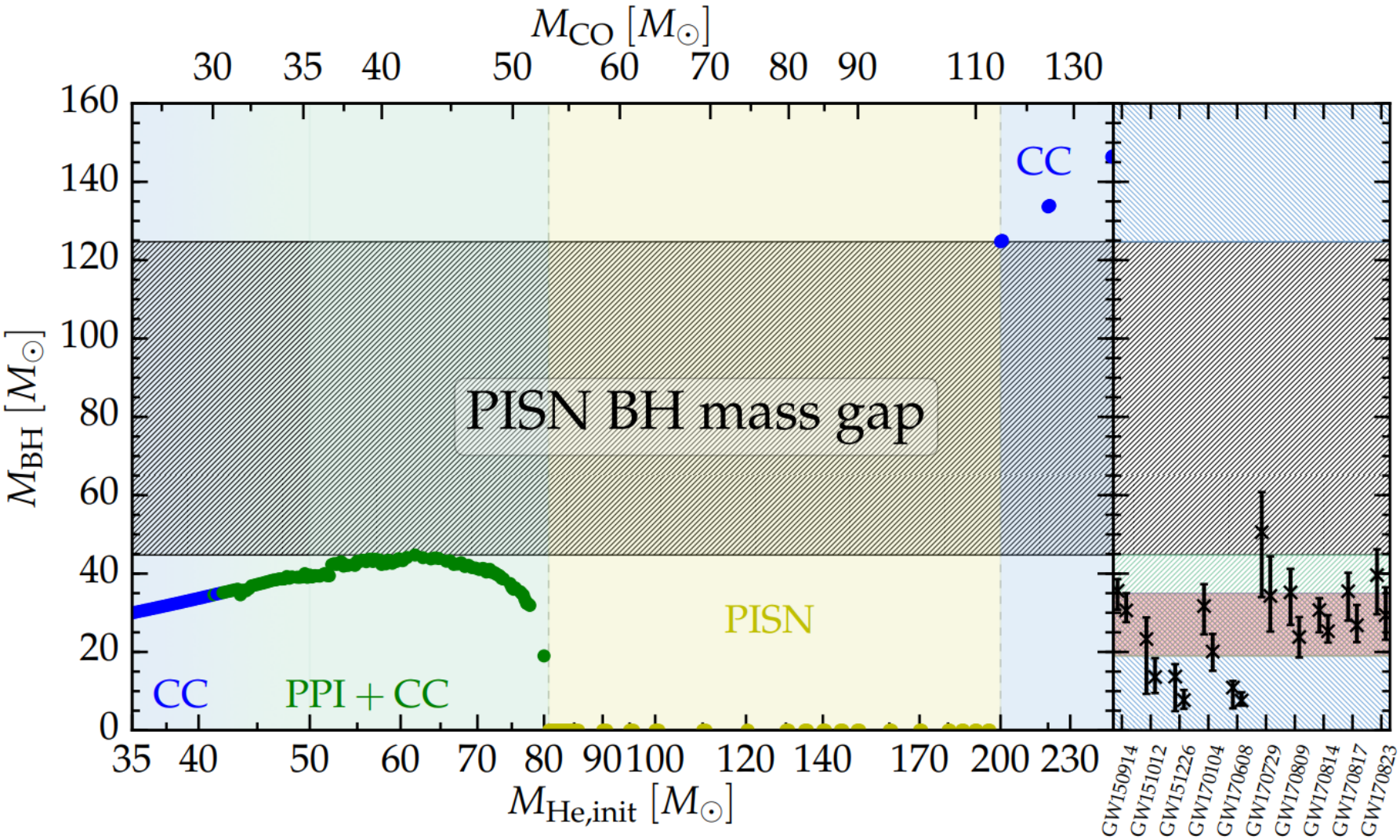

Fig. 2. Final BH masses as a function of the initial He core mass. The scale in the horizontal direction is logarithmic. The colors in the background indicate the approximate range for each evolutionary path, see also Section 3. The right panel shows the masses inferred from the first ten binary BH mergers detected by LIGO/Virgo, with a red shade to emphasize the overlap between PPI and CC, and green and blue hatches to indicate the fate of the progenitor in different BH mass ranges.

Renzo et al. (2020)

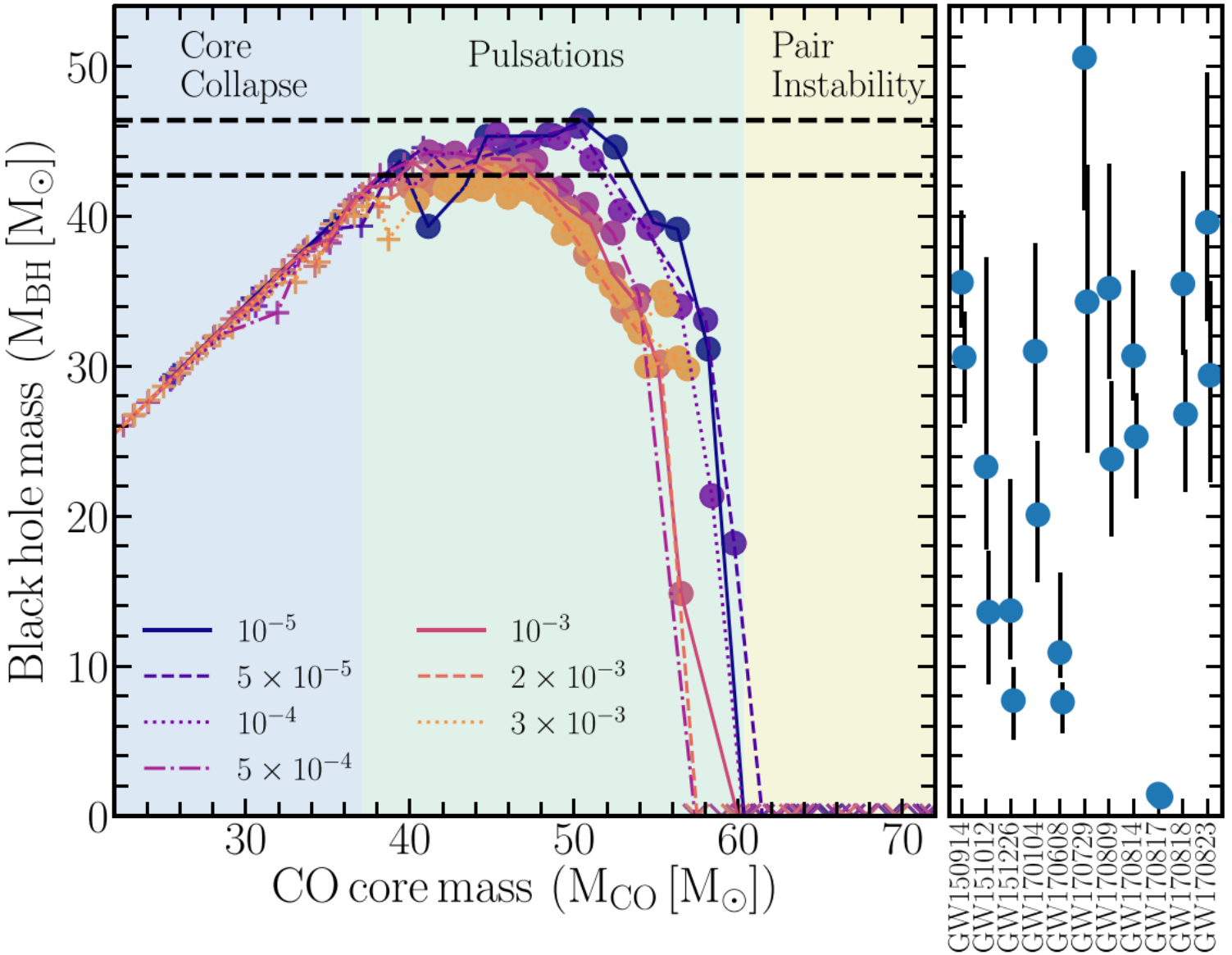

Figure 2. Mass of final BH as a function of the CO core mass for different metallicities. Circles denote models that underwent at least one pulse, pluses evolved directly to CC, and crosses undergo a PISN. The left (blue) region denotes where models undergo CC, the middle (green) region denotes PPISNe, while the right (yellow) region denotes PISNe, as determined by stars with $Z = 10^{-5}$. Points in the right panel show the current median mass estimates for the double compact objects detected by LIGO/VIRGO with their 90% confidence intervals (Abbott et al. 2019a). Dashed horizontal lines emphasize the maximum spread in the locations for the edge of the BH mass gap, or in other words the spread in the maximum BH mass below the PISN BH mass gap.

Farmer et al. (2019)